2015 MERIT Self-directed Joint Research

Construction of sub-cycle pump-probe measurement system using electric-field-waveform-stable mid infrared pulse and measurement of high intensity electric field effect in 2D cuprates

Department of Advanced Materials Science, Graduate School of Frontier Sciences, Takeshi Morimoto
Department of Physics, School of Science, Keisuke Kaneshima

1. About the authors

Takeshi Morimoto (Author#1) is a PhD student at the Advanced Materials Science, the University of Tokyo under the supervision of Prof. Hiroshi Okamoto. His Research theme is ultrafast photo control of electronic states by using an intense terahertz pulse.

Keisuke Kaneshima (Author#2) is a PhD student at the Institute for Solid State Physics of the University of Tokyo under the supervision of Prof. Jiro Itatani. His current research interests include development of ultrafast coherent light sources, attosecond science, and strong-field physics in solids.

2. Background and urpose of research

2.1 Control of the absolute-phase in the electric-field of laser pulse

Since the invention of the laser in 1960, laser technologies are still evolving. Breakthroughs in recent developments of ultrafast laser technologies are (i) Extension of achievable peak intensity, (ii) Expansion of accessible spectral regions, and (iii) Realization of carrier-envelop phase stabilization. Here we introduce (iii), which has close relationship with this self-directed joint research.

In a train of optical pulses from traditional pulsed lasers, the phase between the carrier wave and the position of the intensity envelope (Carrier-Envelope Phase, CEP) is varying from pulse to pulse, as shown in Fig. 1(a). Recent developments of the technologies to detect and control CEP enabled us to keep electric-field oscillations unchanged, as shown in Fig. 2.1(b). Note that the Nobel Prize in physics 2005 was awarded to J. Hall and T. Hänsch for the works related to the CEP-controlling technologies.

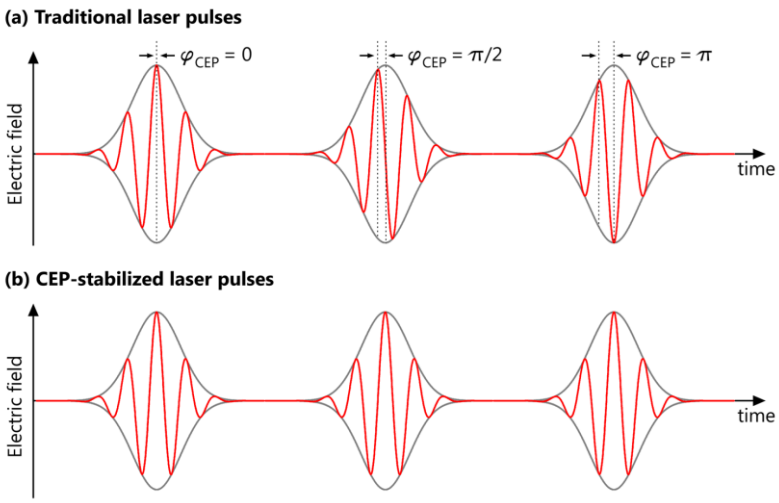

Fig. 2.1. (a) Train of optical pulses from traditional pulsed lasers, (b) Train of optical pulses from CEP-stabilized lasers.

By combining the above technologies including CEP control technique, CEP-stable intense optical pulses whose durations are only below 2 cycles of the electric-field oscillation have become available. Such waveform-controlled intense optical pulses enabled us to manipulate the motions of electron wave packets in high harmonic generation process. As a result, optical pulses in the vacuum ultraviolet (VUV) region with pulse durations of the order of attosecond (10^{-18} sec.) were turned out to be able to be generated via HHG, and ultrafast optics in the attosecond timescale (Attosecond science) is rapidly progressing [1].

In parallel with the extension of ultrafast optics toward shorter wavelength region, the technologies for generating CEP-stable intense THz pulses have also been developed based on the Ti:sapphire laser technology. In particular, tilted-pulse-front pumping technique developed by J. Hebling et al. [2] have enabled us to generate THz electric fields exceeding 1 MV/cm.

2.2 Sub-cycle spectroscopy

In the process of high harmonic generation (HHG) from atoms, the following three steps occur within one optical cycle (Fig. 2.2): (1) Tunnel ionization of an electron by a strong laser electric field; (2) Acceleration of the electron; (3) Recombination of the electron and the parent ion. HHG is a strongly nonlinear phenomenon in the non-perturbative regime, a small variation of an electric field strength changes the generated high harmonic spectrum dramatically. To elucidate such strong-field phenomena that occur within the time scale shorter than one optical cycle and depend not on the pulse envelope but on the waveform itself, we need to prove the sub-cycle response in the time domain.

In attosecond science, the pump-probe spectroscopy employing a CEP-stable NIR pulse that is used to generate attosecond pulse as pump and the generated attosecond pulse as probe can probe the sub-cycle response to the NIR waveform. Such pump-probe spectroscopy combining CEP-stable long-wavelength pump pulses and short-wavelength probe pulses with a pulse duration shorter than one optical cycle of the pump field called *sub-cycle spectroscopy* (Fig. 2.3). Examples of such sub-cycle spectroscopy in attosecond science include *attosecond streaking spectroscopy* [3, 4] and *attosecond transient absorption spectroscopy* [5]. In THz science, sub-cycle spectroscopy can be realized by combining a CEP-stable THz pulse as pump and the NIR pulse that is used to generate the THz pulse as probe. Examples of sub-cycle spectroscopy in THz science include electro-optic sampling (EO sampling) [6] and THz-Pump/Optical-Probe spectroscopy.

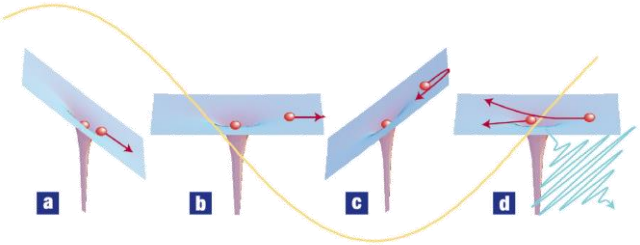

Fig. 2.2. HHG from atoms [3]. The yellow curve shows the laser electric field. (a)-(b) An intense NIR electric field ionizes an electron from an atom and accelerates it away into free space. (c) When the electric field changes direction, the electron turns around and accelerates back towards the parent ion, gaining a substantial amount of kinetic energy in the process. (d) Electron recombines with the parent ion and the excess amount of kinetic energy is released as a single high-energy photon.

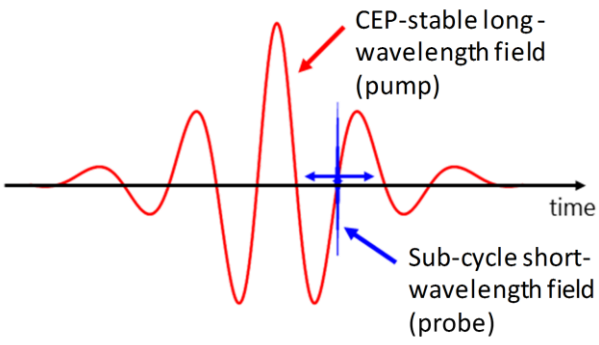

Fig. 2.3. Concept of sub-cycle spectroscopy.

2.3 Motivations for the generation of CEP-stable intense MIR pulses and the self-directed joint research.

As a progress of the technologies for intense THz pulse generation, the novel area of science focusing on strong-field processes in solids is being actively studied [7, 8]. By using intense low-frequency optical fields with photon energy much lower than the band gap energies of solids, extreme nonlinear responses and novel transient phases are expected to emerge in strongly-driven electronic states.

THz pulses can produce a field strength of more than 1 MV/cm [3], mid-infrared (MIR) pulses can produce much stronger fields because of their better focusability and possibly shorter pulse duration. Thus far, the generation of carrier-envelope phase (CEP)-stable pulses in the MIR region with a field strength of more than 100 MV/cm has been reported [9]. By applying such a strong electric field that almost break a semiconductor crystal (~few tens of MV/cm), HHG from solids which originate in Bloch oscillation has begun to be observed [10, 11].

An intense MIR and THz laser system that has a capability for sub-cycle spectroscopy is essential to advance the studies about strong-field physics in solids. As mentioned above, the technique for THz pulse generation by J. Hebling et al. [2] enables us to construct sub-cycle spectroscopy system using intense and CEP-stable THz pulse. On the other hand, the realization of MIR laser system that has a capability for sub-cycle spectroscopy is not easy due to following reasons.

(1) Generation of CEP-stable intense MIR pulses requires a complicated setup that consists of multiple OPAs.

(2) Since optical cycle of MIR waves are faster than that of THz waves, a much shorter pulse duration of probe pulses is required for sub-cycle probing. For example, one optical cycle of MIR light with a wavelength of 9 μm is 30 fs.

Author#2 has succeeded to generate CEP-stable intense MIR pulse and ultrashort visible pulse, and overcame the challenges (1) and (2) (mentioned at section 3.1). On the other hand, author#1 has ever been working on photo control of property of solids including strongly correlated electron system using a CEP-stable intense terahertz pulse. We have considered that collaboration with each other enables a novel research, which means that we use a CEP-stable intense MIR pulse as an excitation pulse and observe ultrafast responses in strongly correlated electron systems by sub-cycle spectroscopy. This motivation leads us to the self-directed joint research.

3. Materials and methods

3.1 Optic system of CEP-stable intense MIR pulse and ultrashort visible pulse

In order to overcome the above challenge (1), Author #2 et al. proposed and demonstrated a novel scheme of OPA named *dual-wavelength OPA*. By employing this scheme, CEP-stable intense MIR pulses with a peak electric field strength exceeding 50 MV/cm were generated [12]. In addition, Author #2 et al. succeeded in the generation of 5-μJ, 6.5-fs visible pulses using filamentation in a gas cell filled with krypton followed by spectral selection and phase compensation by a combination of dielectric mirrors, and the challenge (2) was also overcome [13].

Fig. 3.1. shows the schematic of the experimental setup. The details of the system are described in [12] and not explained here. One of the characteristics of the system is wavelength-selective amplification using material dispersion and broadband OPAs (dual-wavelength OPA), which enables efficient, tunable, and stable MIR pulse generation (5-11 μm, 5 μJ, 70 fs, 1 kHz) as shown

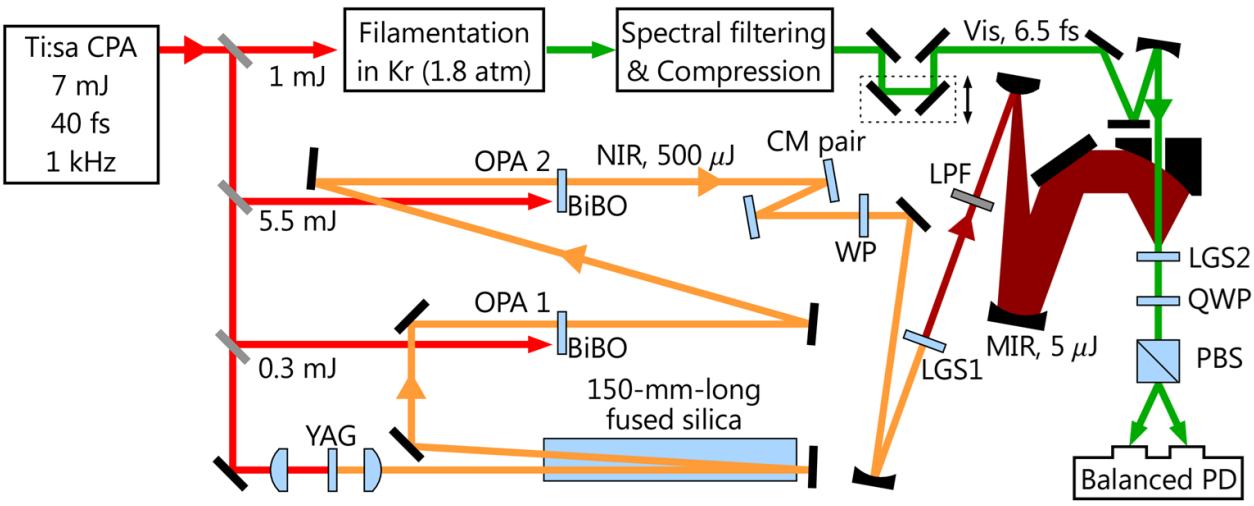

Fig. 3.1. Schematic of the experimental setup [12]. YAG; 4-mm-thick YAG crystal, BiBO; 1-mm-thick BiB_3O_6 crystals, CM pair; a pair of broadband NIR chirped mirrors, WP; waveplate, LGS1; 1-mm-thick $LiGaS_2$ crystal, LPF; low-pass filter, LGS2; 15-μm-thick $LiGaS_2$ crystal, QWP; quarter waveplate, PBS; polarizing beam splitter.

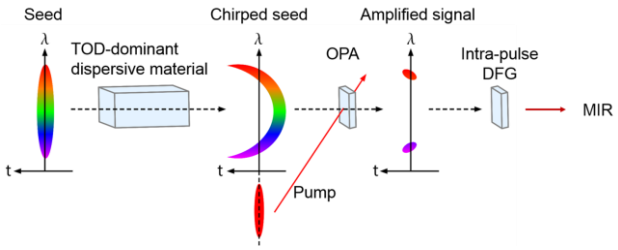

Fig. 3.2 Concept of the dual-wavelength OPA.

in Fig. 3.2. The radius of $1/e^2$ intensity of the MIR beam was measured by a knife-edge method to be 32 μm, corresponding to a peak electric field amplitude of 56 MV/cm at the focal point of the off-axis parabolic mirror.

3.2 2D Cuprates

In this section we discuss about target materials of MIR pulse excitation, 2D cuprates: Nd_2CuO_4 (NCO) and $Sr_2CuO_2Cl_2$ (SCOC). 2D cuprates are well known as superconductor (electron- or hole-doped). On the other hand, it is interesting as Mott insulators (non-doped). Fig. 3.3 shows crystal structures of NCO and SCOC. In these materials, CuO2 planes ,which is 2D planes composed by Cu and O, are important for electronic property. Copper atoms are surrounded by 4 oxygen atoms in NCO and 6 oxygen atoms in SCOC, respectively. In these compounds, the Mott-Hubbard gap opens in the *d* band of copper due to the large on-site Coulomb interactions at copper sites, and the occupied *p* band of oxygen is located between the upper and lower Hubbard bands of copper. Thus, the lowest optical excitation is charge transfer (CT) transition from the oxygen 2p valence band to the copper 3d upper Hubbard band (Fig. 3.4)

The reason why 2D cuprates has chosen as the target materials is that large optical response resulting from strong electron correlation is expected in the energy region of the using probe pulse. In this experiment, photon energy of the probe pulse is fixed as the expense of ultrashort pulse duration. Therefore, large optical response should be observed in the energy region the of probe pulse (1.5 ~ 2.5 eV). Mott gap of NCO and SCOC are located at 1.5 ~ 2 eV as shown Fig. 3.5., and there is a high possibility of large optical responses by MIR pulse in this energy region. Indeed, when a terahertz

pulse is used as a pump pulse, reflectivity change which time evolution accord with the square of the waveform of the terahertz electric-field is observed around the Mott gap (Fig. 3.6., [14]). This response can be understood as third order nonlinear optical response caused by the terahertz electric-field. From this previous study, it can be considered that MIR pulse also cause large optical response around Mott gap.

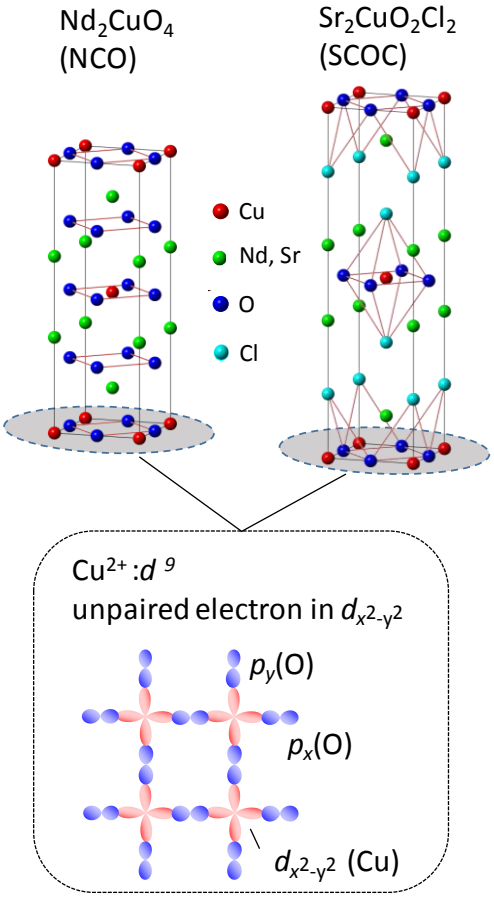

Fig. 3.3. Crystal structure of NCO and SCOC.

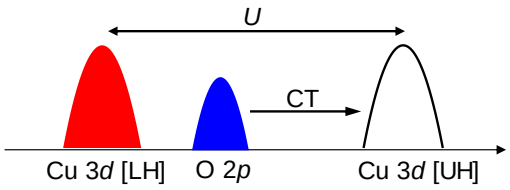

Fig. 3.4 Simple Band structure of NCO and SCOC.

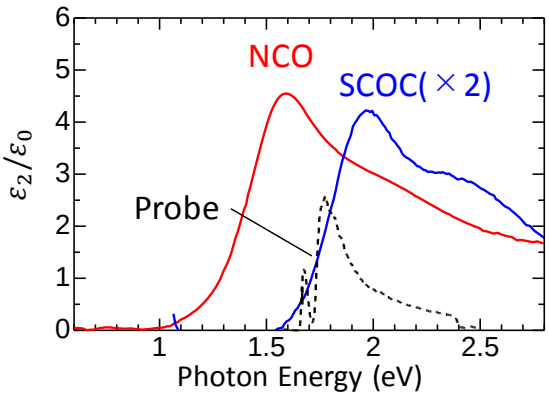

Fig. 3.5. ε_2 spectrum of NCO and SCOC (solid line), spectrum of the probe pulse (broken line).

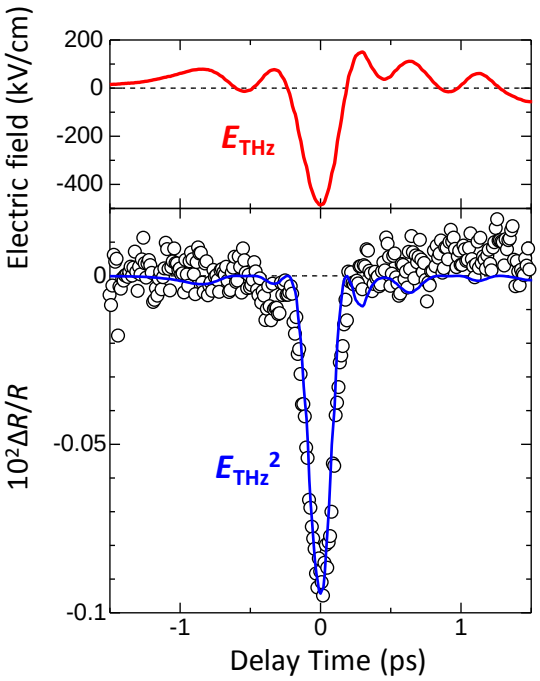

Fig 3.6. (Upper panel) electric-field waveform of the pump terahertz pulse. (Lower panel) Reflectivity change induced by the terahertz pulse (circle) and square of the electric-field waveform of the pump terahertz pulse (blue line).

3.3 Pump-probe spectroscopy and EO sampling

This section describes pump-probe spectroscopy, which is main experimental method in this research, and EO sampling, which is the method to measure electric-field waveform of MIR pulse. Fig. 3.7 shows concept of pump-probe spectroscopy. In this method, sample is excited by pump pulse, and then reflectivity or

transmission change resulting from changes of electronic/lattice/spin systems are observed by probe pulse. Time evolution of the systems can be observed by changing the path length of light. In the same experimental setup, we can perform Electro-Optic sampling (EO sampling) and measure the electric-field waveform of the MIR pulse by replacing the sample for nonlinear optical crystal (EO crystal). At the EO sampling, MIR pulse changes the refractive index of the EO crystal, and then, polarization of probe pulse (sampling pulse) transmitting the EO crystal also changes. We can detect the signal resulting from polarization change and measure the electric-field waveform of the MIR pulse directly. EO sampling is widely used to measure the electric-field waveform of the THz pulse [6]. It is necessary to use ultrashort pulse which duration is shorter than the period of the MIR electric-field in order to apply this method to the MIR pulse. In this research, 6.5 fs ultrashort visible pulse is used as the sampling pulse, which is also used for pump-probe spectroscopy in the cuprates.

4. Experimental results and consideration

This section describes the results obtained in the self-directed joint research. Section 4.1 describes the electric-field waveform of the MIR pulse measured by

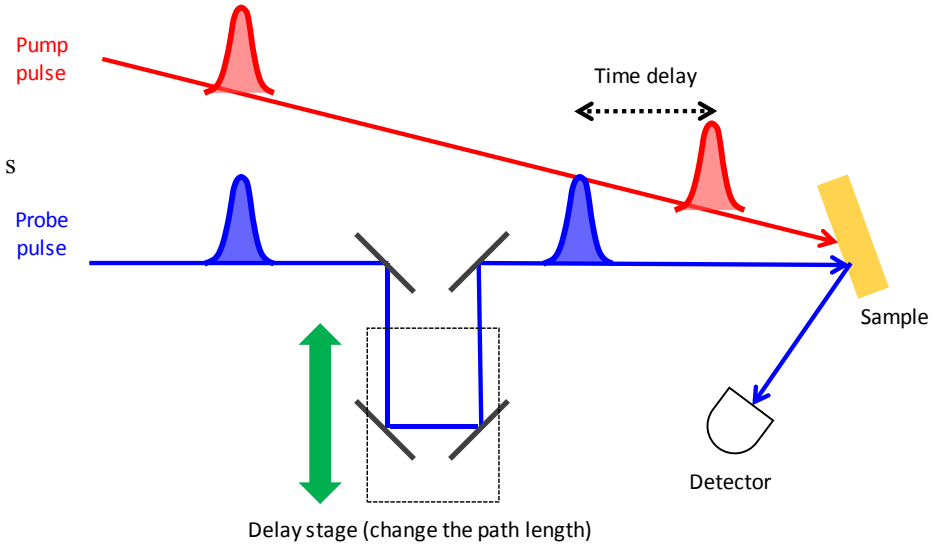

Fig. 3.7. Experimental setup for pump-probe spectroscopy.

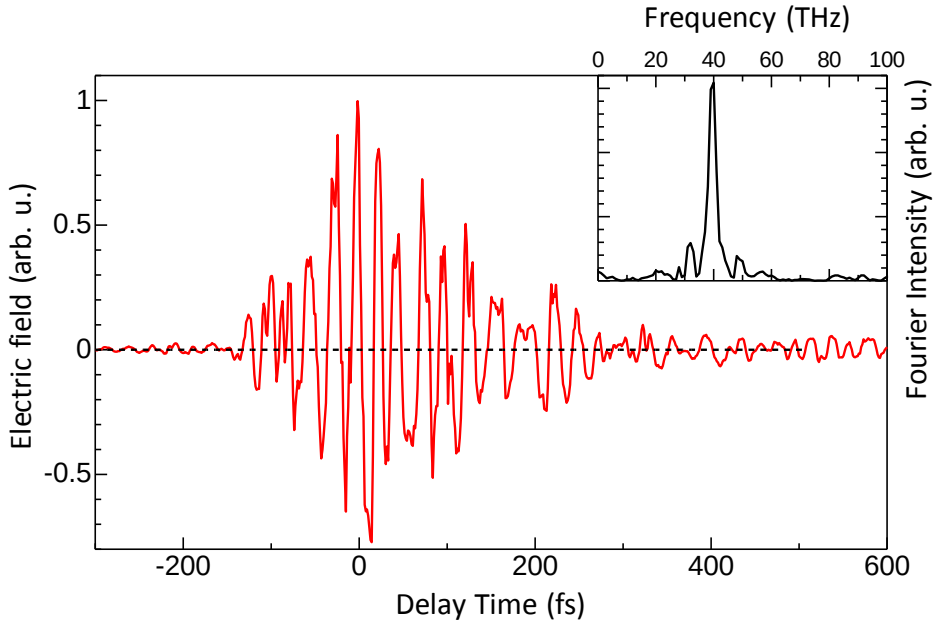

Fig. 4.1 The electric-field waveform of the MIR pulse measured by EO sampling. Inset shows Fourier transformation of the electric-field waveform.

EO sampling. Section 4.2 and 4.3 describes the results of the pump-probe spectroscopy using MIR as the pump pulse in the SCOC and NCO, respectively.

4.1 EO sampling

Fig. 4.1 shows the electric-field waveform of the MIR pulse obtained by EO sampling. The most important thing is that we have successfully measured the electric-field waveform. In the case of an CEP-unstable pulse, signals in the EO sampling are cancelled out due to the integration of the signals from all pulses. Therefore, this results guarantee the generation of the CEP-stable MIR pulse. In addition, the sampling pulse used for EO sampling is ultrashort visible pulse, which is also used for pump-probe spectroscopy in the 2D cuprates. Thus, this success in the EO sampling means that fundamental setup for pump-probe spectroscopy has already prepared at this stage.

The electric-field waveform in the Fig. 4.1 shows that period of the MIR pulse is about 26 fs, and pulse width is about 80 fs (FWHM of the intensity). Fourier transformation of the electric-field (Inset) indicates that the central frequency of the MIR pulse is about 40 THz (0.16 eV). This MIR pulse generation system constructed by author#2 can change the central frequency of the MIR pulse. However, in this research, frequency dependence of the pump pulse was not measured and we fix the central frequency of the MIR pulse at 40 THz. The electric-field waveform of the MIR pulse shown in the Fig. 4.1 is a typical one and detail of the wave form changes by alignment of the optics. So we performed EO sampling every time before pump-probe spectroscopy in the 2D cuprates.

Finally, we discuss about peak electric-field intensity of the MIR pulse. We discussed about it in the section 3.1 but the condition in this self-directed joint research is slightly different. In the pump-probe spectroscopy of NCO and SCOC, pulse energy of the MIR pulse is about 2 μJ (per pulse) at the focal point、and the dimeter is about 32 μm (FWHM). From these value and the

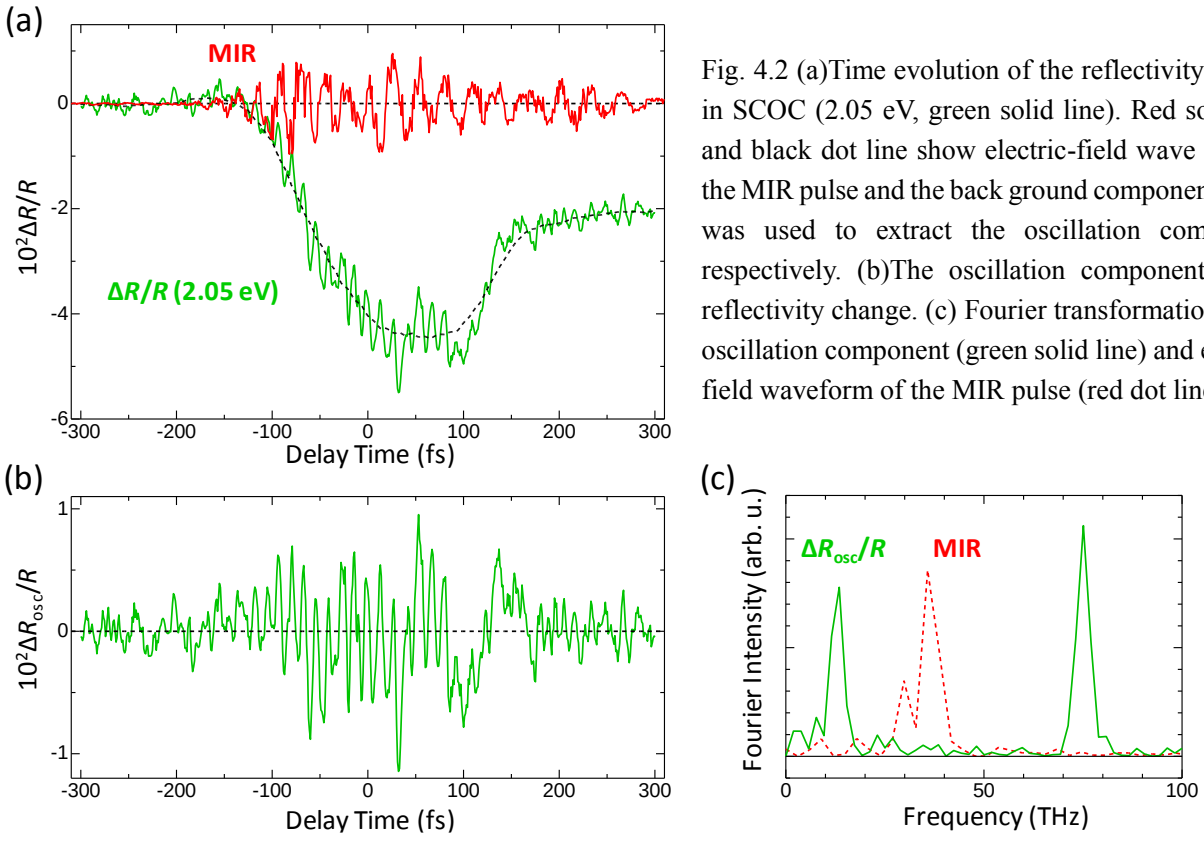

Fig. 4.2 (a)Time evolution of the reflectivity change in SCOC (2.05 eV, green solid line). Red solid line and black dot line show electric-field wave form of the MIR pulse and the back ground component which was used to extract the oscillation component, respectively. (b)The oscillation component in the reflectivity change. (c) Fourier transformation of the oscillation component (green solid line) and electric-field waveform of the MIR pulse (red dot line).

electric field waveform, we can estimate that peak intensity of the MIR electric-field is about 33 MV/cm, which is 100 times larger than that of the THz pulse used in previous research [14].

4.2 MIR pulse excitation in SCOC

Fig 4.2 (a) shows a time evolution of the MIR pulse induced reflectivity change in SCOC (green solid line). Probe energy is set to 2.05 eV by inserting a band pass filter in front of a photo detector. In Fig. 4.2., the electric-field waveform of the MIR pulse is also shown. A broad negative reflectivity change was observed simultaneously with the MIR pulse irradiation. In addition to the broad reflectivity change, there exists a sharp oscillation structure from -100 fs to +100 fs. We subtracted background signal, which is shown black broken line, from the entire signal to extract this oscillation component. The extracted oscillation component is shown in the Fig. 4.2 (b). Fig 4.2. (c) is a Fourier transformation (-200 fs ~ +300 fs) of the oscillation component (solid green line). In the same figure, Fourier transformation of the MIR pulse is also shown (red dotted line). The Fourier transformation indicates that oscillation components which frequency is 13 THz and 75 THz are included in the reflectivity change. Among them,75 THz is twice as much as the 36 THz, which is the central frequency of the MIR pulse. Such an oscillation which period is shorter than that of excitation pulse can be observed only when a CEP stable pump pulse and ultrashort probe pulse is used for the measurement. In this sense, observation of this 75 THz oscillation exhibits the success in the demonstration of the sub-cycle spectroscopy. Another oscillation is discussed later in the section 4.3.

Figure 4.3 shows the probe energy dependence of the reflectivity change which was measured by bandpass filters. At the all probe energy, broad reflectivity changes which is generated simultaneously with MIR pulse irradiation. Sign of the reflectivity changes is negative in the low energy region, and positive in the high energy region. In the figure 4.4 (b), we show the reflectivity change spectrum, which was obtained by plot of the peak value in the fig 4.3 (red circles). The reflectivity change at 2.11 eV is excluded because its sign is different at each time region. Blue circles show reflectivity change spectrum at the previous research of THz pump. The reflectivity (black solid line) and ε_2 (red solid line) of SCOC on the steady state and the spectrum of the probe pulse (black dot line) are also shown in fig 4.3 (a). THz wave excitation causes the reflectivity change whose sign is positive, negative, positive from low energy region to high energy region around the Mott gap. The reflectivity change spectrum caused by the MIR pulse is similar to that is cause by

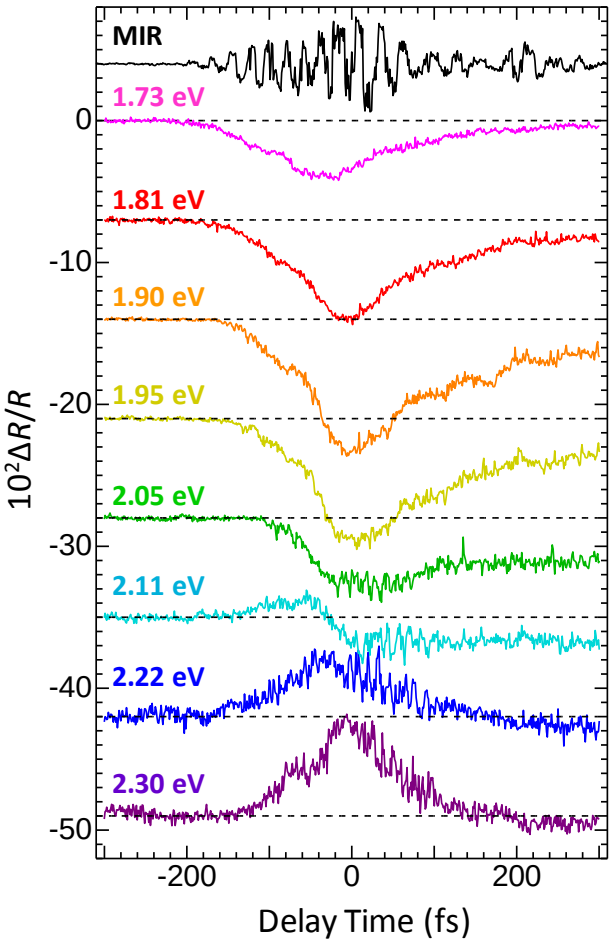

Fig. 4.3 The probe energy dependence of the reflectivity change in the SCOC.

the THz wave. However, time evolution of the reflectivity changes is extremely different with each other. As shown in the fig. 3.6, time evolution of the reflectivity change by the THz wave pump perfectly accords with the square of the electric-field waveform of the THz wave. On the other hand, time evolution of the reflectivity change by the MIR pulse pump has broad shape, which is similar not to the square of the electric-field waveform but to the envelope of the MIR pulse. The aforementioned oscillation component possibly corresponds to the square of the electric-field waveform of the MIR pulse because its frequency is twice of the frequency of the MIR pulse. However, this oscillation is observed only in the high energy region (2.05 ~ 2.30 eV). This is different result with the THz pump measurement, where the reflectivity change corresponding to the square of the electric-field waveform was observed at the all energy region.

Taking these result into consideration, the reflectivity change by the MIR pulse can originate from new mechanism which is different from the third order nonlinear optical effect. The reason of such a reflectivity change is still not clear. Additional experiment which will be discussed in the "5. Summary and Future plan" can give further information.

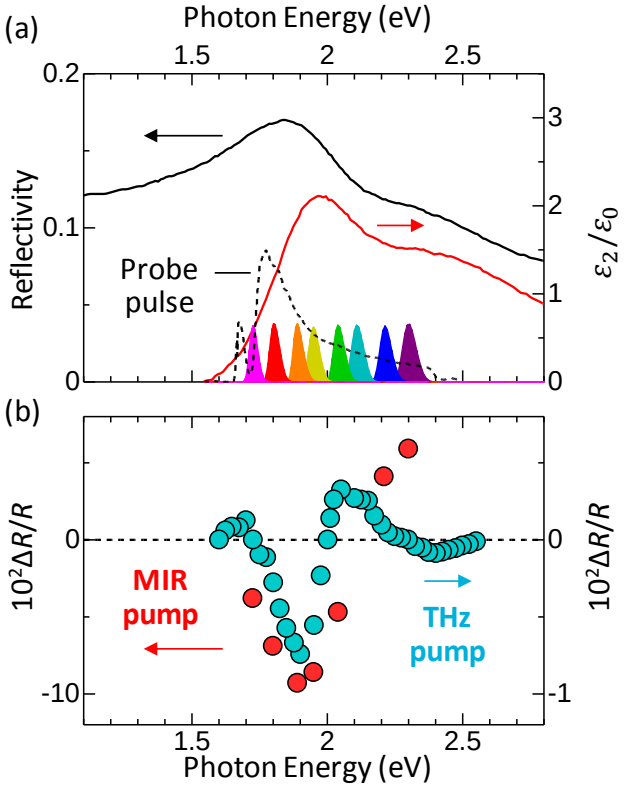

Fig. 4.4 (a) Reflectivity spectrum (black solid line) and $\boldsymbol{\varepsilon_2}$ spectrum (red solid line) of the SCOC. Black dot line shows the spectrum of the probe pulse. Shaded diagrams show the spectrum of the bandpass filters. (b) The reflectivity change spectrum by the MIR pulse pump (red circles). Blue circles show reflectivity change spectrum by the THz wave pump.

4.3 MIR pulse excitation in NCO

Time evolution of the reflectivity changes by the MIR pulse in the NCO are shown in the fig. 4.5. In the NCO, the reflectivity changes are not vanished after the electric-field component of the MIR pulse is vanished, which is different from the reflectivity changes in the SCOC. Then, fig. 4.6 (b) shows the reflectivity change spectrum (red circles). In the same way as in SCOC, the reflectivity change spectrum by the THz wave excitation (blue circles), reflectivity spectrum (black line) and ε_2 spectrum (red line) are also shown in fig 4.6. MIR pulse excitation causes negative reflectivity change in the all energy region measured in this experiment. This result indicates that the mechanism of the reflectivity change in the NCO is different from that in the SCOC.

A possible phenomena observed in the NCO is carrier generation by the pump pulse and insulator-to-metal transition. In the 2D cuprates including NCO, pulse excitation whose photon energy exceeds Mott gap generates carriers and causes ultrafast insulator-to-metal transition [15]. At that time, absorption of the Mott gap decreases by the carrier generation and negative reflectivity changes were observed around the Mott gap.

This result is confirmed by the pump-probe measurement with using 7 fs visible pulse in the laboratory where author#1 belongs to [16]. Taking this previous research into account, MIR pulse may cause carrier excitation in this research.

We should consider that the photon energy of the MIR pulse used in this experiment is about 0.16 eV and it is much smaller than Mott gap of the NCO (~1.5 eV). Usually, excitation in the transparent energy region cannot generate carrier. However, in such a situation, it is predicted theoretically that extreme strong electric-field can generate carrier through a process called tunneling ionization [17]. Fig. 4.7 shows the concept of the tunneling ionization. Intense electric-field causes spatial gradient of the band and electron (or hole) tunnels between the upper band and lower band. Experimentally, there are reports of the tunneling ionization by the intense THz pulse and MIR pulse in the Mott insulator, VO_2 [18,19]. Required electric-field intensity for the tunneling ionization is related with correlated length between doubloon and hole or energy of the Mott gap. The theoretical research [17] predicts that threshold electric-filed is 3 ~ 16 MV/cm in the some 1D Mott insulator. Although NCO is a 2D Mott insulator, it can be considered that intense electric-filed used in this research (33 MV/cm) can cause tunneling ionization.

Finally, we reconsider the results in the SCOC in terms of carrier generation. In fig. 4.3, we can find negative reflectivity change after +200 fs in the all energy region.

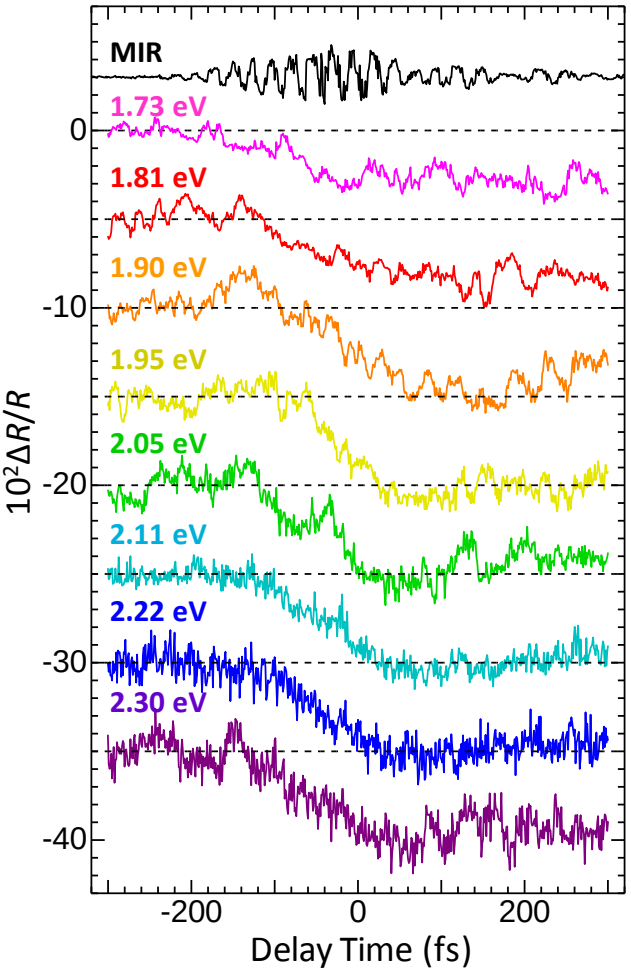

Fig. 4.5 The probe energy dependence of the reflectivity change in the NCO.

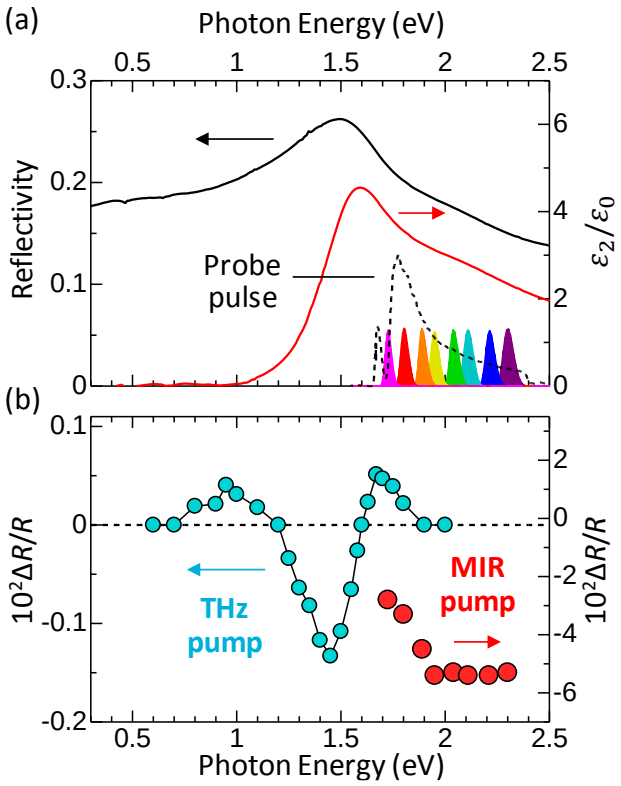

Fig. 4.6 (a) Reflectivity spectrum (black solid line) and $\boldsymbol{\varepsilon_2}$ spectrum (red solid line) of the SCOC. Black dot line shows the spectrum of the probe pulse. Shaded diagrams show the spectrum of the bandpass filters. (b) The reflectivity change spectrum by the MIR pulse pump (red circles). Blue circles show reflectivity change spectrum by the THz wave pump.

This indicates possibility of the carrier generation also in SCOC. Furthermore, oscillation shown in the fig. 4.2 (c) (13 THz) is considered to be a coherent oscillation of phonon which is caused by the interaction between carrier and phonon. The reason of weak carrier generation in SCOC, compared to that in NCO, can be attributable to the smaller band gap of SCOC than that of NCO.

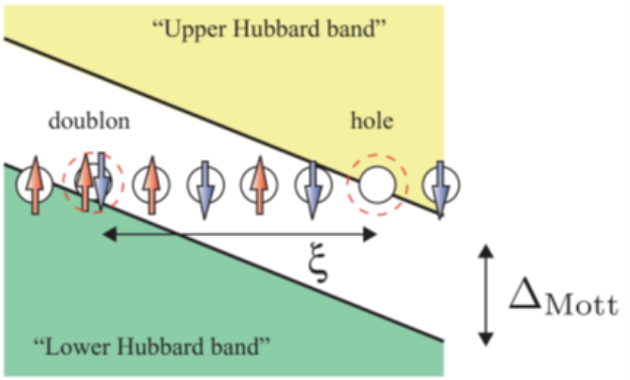

Fig. 4.7 Schematic of tunneling ionization in strong dc electric-fields [17].

5. Summary and Future plan

The purpose of this self-directed joint research was to construct sub-cycle pump-probe measurement system with using CEP stable intense MIR pulse and visible ultrashort pulse which had been made by Author#2 and to apply it to electron correlated systems. Firstly, we constructed the pump-probe measurement system and succeeded to measure the electric-field waveform of the MIR pulse. Secondly, we performed MIR pump-visible probe measurement (sub-cycle spectroscopy) in the 2D cuprates, SCOC and NCO. In SCOC, the reflectivity change was observed, whose sign was positive in the higher energy region than energy of the Mott gap, and negative in the lower energy region. In addition, coherent oscillation whose frequency is twice of the MIR pulse frequency was observed in the reflectivity change in the higher energy region. Detection of such a short period oscillation which period is shorter than that of the electric-field of the pump pulse is not possible without sub-cycle spectroscopy. In that context, this self-directed joint research is very meaningful. Although the origin of the reflectivity change and coherent oscillation in SCOC is unclear at present, it can be considered that these phenomena are different from conventional third order nonlinear optical response, which was observed by the THz wave pump because time evolution of the reflectivity changes are completely different. On the other hand, negative reflectivity change in all (measured) energy region was observed in NCO. This reflectivity change, which is equal to the absorption decrease at the Mott gap, indicates carrier generation by the MIR pulse excitation. Possible mechanism of carrier generation is tunneling ionization because photon energy of the MIR pulse is much smaller than energy of the Mott gap. Tunneling ionization is a non- perturbative phenomenon which is caused by quite intense electric field (several tens MV /cm) and there are a few reports about this phenomenon. As mentioned above, it can be said that we successfully observed new response which has never been observed in 2D cuprates by using CEP-stable intense MIR pulse and sub-cycle spectroscopy system. A next problem is to clarify the mechanism of such new responses. One of the necessary measurement is electric-field intensity dependence of the MIR pulse. Although we cannot perform this measurement in this research, electric-field intensity dependence has important information. Especially, if tunneling ionization occurs in NCO, the reflectivity change should show huge nonlinearity to the intensity of the MIR pulse. Furthermore, a measurement of the reflectivity spectrum in wider region is also effective. Although such a measurement is possible by widely-used OPA, we cannot perform sub-cycle probe measurement by such a OPA because the duration of the probe pulse become longer than ultrashort visible pulse which we used. However, since background signal of

the reflectivity changes caused by the MIR pulse excitation is relatively broad, we can get a certain amount of information by using normal OPA system. It can be considered that such a measurement can reveal the origin of the reflectivity change in SCOC, which is unclear only in this research.

6. Acknowledgment

We would like to thank Prof. Hiroshi Okamoto, Prof. Jiro Itatani, and Prof. Kyoko Ishizaka for permitting this research. Finally, we express great gratitude to the MERIT program for giving us this valuable opportunity of research.

7. References

[1] P. B. Corkum and F. Krausz, "Attosecond science," Nat. Phys. **3**, 381 (2007).

[2] J. Hebling, G. Almási, I. Z. Kozma, and J. Kuhl, "Velocity matching by pulse front tilting for large-area THz-pulse generation," Opt. Express **10**, 1161 (2002).

[3] J. Itatani, F. Quéré, G. L. Yudin, M. Yu. Ivanov, F. Krausz, and P. B. Corkum, "Attosecond Streak Camera," Phys. Rev. Lett. **88**, 173903 (2002).

[4] E. Goulielmakis, M. Uiberacker, R. Kienberger, A. Baltuska, V. Yakovlev, A. Scrinzi, Th. Westerwalbesloh, U. Kleineberg, U. Heinzmann, M. Drescher, and F. Krausz, "Direct Measurement of Light Waves," Science **27**, 1267 (2004).

[5] M. Schultze, K. Ramasesha, C.D. Pemmaraju, S.A. Sato, D. Whitmore, A. Gandman, J. S. Prell, L. J. Borja, D. Prendergast, K. Yabana, D. M. Neumark, and S. R. Leone, "Attosecond band-gap dynamics in silicon," Science **12**, 1348 (2014).

[6] Q. Wu and X. C. Zhang, "Ultrafast electro-optic field sensors," Appl. Phys. Lett. **70**, 1604 (1996).

[7] T. Kampfrath, K. Tanaka, and K. A. Nelson, "Resonant and nonresonant control over matter and light by intense terahertz transients," Nat. Photon. **7**, 680 (2013).

[8] S. Ghimire, G. Ndabashimiye, A. D. DiChiara, E. Sistrunk, M. I. Stockman, P. Agostini, L. F. DiMauro, and D. A. Reis, "Strong-field and attosecond physics in solids," J. Phys. B **47**, 204030 (2014).

[9] A. Sell, A. Leitenstorfer, and R. Huber, "Phase-locked generation and field-resolved detection of widely tunable terahertz pulses with amplitudes exceeding 100 MV/cm," Opt. Lett. **33**, 2767 (2008).

[10] S. Ghimire, A. D. DiChiara, E. Sistrunk, P. Agostini, L. F. DiMauro, and D. A. Reis, "Observation of high-order harmonic generation in a bulk crystal," Nat. Phys. **7**, 138 (2011).

[11] O. Schubert, M. Hohenleutner, F. Langer, B. Urbanek, C. Lange, U. Huttner, D. Golde, T. Meier, M. Kira, S. W. Koch, and R. Huber, "Sub-cycle control of terahertz high-harmonic generation by dynamical Bloch oscillations," Nat. Photon. **8**, 119 (2014).

[12] K. Kaneshima, N. Ishii, K. Takeuchi, and J. Itatani, "Generation of carrier-envelope phase-stable mid-infrared pulses via dual-wavelength optical parametric amplification," Opt. Express **24**, 8660 (2016).

[13] K. Kaneshima, N. Ishii, and J. Itatani, "Generation of spectrally-stable 6.5-fs visible pulses via filamentation in krypton," High Power Laser Sci. Eng. (submitted)

[14] T. Terashige *et al*., In preparation

[15] H. Okamoto, T. Miyagoe, K. Kobayashi, H. Uemura, H. Nishioka, H. Matsuzaki, A. Sawa, and Y. Tokura, "Photoinducedtransition from Mott insulator to metal in the undoped cuprates Nd_2CuO_4 and La_2CuO_4," Phys. Rev. B **83**, 125101 (2011).

[16] T. Miyamoto, Y. Matsui, T. Terashige, N. Osawa, Y. Miyata, H. Yada, Y. Watanabe, S. Adachi, T. Ito, K. Oka, B. –S. Li, A. Sawa, and H. Okamoto, "Probing ultrafast photocarrier relaxation via emission of magnons in the

cuprate Mott insulator Nd_2CuO_4," In preparation.
[17] T. Oka, "Nonlinear doubloon production in a Mott insulator: Landau-Dykhne method applied to an integrable model" Phy. Rev. B **86**, 075148 (2012).
[18] Mengkun Liu, Harold Y. Hwang, Hu Tao, Andrew C. Strikwerda, Kebin Fan, George R. Keiser, Aaron J. Sternbach, Kevin G. West, Salinporn Kittiwatanakul, Jiwei Lu, Stuart A.Wolf, Fiorenzo G. Omenetto, Xin Zhang, Keith A. Nelson, and Richard D. Averitt, "Terahertz-field-induced insulator-to-metal transition in vanadium dioxide metamaterial" Nature **487**, 345 (2012).
[19] B. Mayer, C. Schmidt, A. Grupp, J. Buhler, J. Oelmann, R. E. Marvel, R. F. Haglund, Jr., T. Oka, D. Brida, A. Leitenstorfer, and A. Pashkin, "Tunneling breakdown of a strongly correlated insulating state in VO_2 induced by intense multiterahertz excitation" Phy. Rev. B **91**, 235113 (2015).